Vol 18 No 3, March 2009
1674-1056/2009/18(03)/1181-07
Chinese Physics B
© 2009 Chin. Phys. Soc.
and IOP Publishing Ltd

Structure and bonding properties of Y doped Σ37 grain boundary in alumina*

Wang Ya-Bin(王亚斌)[a], Zhang Gang(张 刚)[b], Liu Ming-Jie (刘明杰)[a],
Chen Xiang-Long(陈湘陇)[b], and Chen Jun(陈 军)[c]†

[a] *School of Aerospace Science and Engineering, Beijing Institute of Technology, Beijing* 100081, *China*
[b] *China Aerospace Engineering Consultation Center, Beijing* 100037, *China*
[c] *Institute of Applied Physics and Computational Mathematics, Beijing* 100083, *China*

(Received 22 July 2008; revised manuscript received 20 December 2008)

The microscopic structures and the bonding properties of Y-doped and undoped $(01\bar{1}8)/[04\bar{4}1]/180°$ (Σ37) grain boundaries in alumina are investigated by using *ab initio* method. The formation energy of grain boundary and the segregation energy of Y to grain boundary are acquired. Electronic structures, potential distributions, bond orders and effective charges of Y-doped and undoped Σ37 GB systems are calculated. Our results reveal that the higher strength Y–O bond than Al–O bond is ascribed to the hybridization of Y(4p, 3d) with O(2s). Meanwhile, dopant Y also causes a change in potential distribution in the grain boundary region, thereby further affecting the transport property of ceramic alumina.

Keywords: grain boundary, alumina, Y doping, *ab initio* method
PACC: 6170N, 6170R, 7115A

1. Introduction

Alumina (α-Al_2O_3), because of its outstanding high-temperature mechanical property and stable chemical properties in oxidation environments, has been widely used as structural ceramic materials. To a large extent, the macroscopic properties of alumina are controlled by the inner microscopic structures such as grain boundaries (GBs).[1−5] It has been found experimentally that the rare-earth metal dopants, such as Y, La, Zr, etc, can greatly improve the mechanical property of ceramic alumina.[5,6] For example, the doped iso-valence metal Y or La can reduce the creep rate of alumina by 2-3 orders of magnitude.[7,8] This is so-called 'Y-effect' in alumina. Because of their low solubility in bulk α-Al_2O_3, dopants should be segregated to the GBs.[3−9] A lot of research efforts have focused on the Y-effect, but no microscopic theory exists to successfully explain it. Experimentally, a variety of experimental instruments have been developed to investigate the structure environments of the GB in α-Al_2O_3 and the segregation of dopant, such as Auger electron microscopy,[4] x-ray photoelectron spectroscopy (XPS),[5] extend x-ray absorption fine structure (EXAFS),[10] analytical TEM (ATEM),[11] scanning TEM (STEM),[12,13] and electron energy loss spectroscopy (EELS).[13] By using STEM, Bruley *et al* [13] revealed that Y and La ions were segregated into a narrow region of the GB. Gemming *et al* discovered that different GB models had different concentrations of Y substituting Al in a GB region, and some bulk-likely GB models were not sensitive to segregation of dopant.[11] According to the experimental observation of impurity diffusion,[14−16] Cho *et al* suggested that the improvement on creep rate of ceramic alumina by doped Y or La was due to a site-blocking effect of oversized Y or La ions.[14,15] Theoretically, on the other hand, little theoretical research on the ceramic alumina has been carried out. This may be due to the complexity in GB structure of alumina[17−24] as will be discussed in Section 2. Ching and Xu[18] studied the electronic structure and bonding in a crystalline Y–Al–O system, such as α-Al_2O_3, $Y_3Al_5O_{12}$, Y_2O_3, etc. They found that relative bond strengths of Y–O and Al–O bonds in different crystals were significantly dependent on the details of local atomic environments. Elsasser *et al* [19,20] have carried out a series of calculations by using a mixed-basis pseudo-potential method on rhombohedral GB models Σ7 and Σ3 in α-Al_2O_3. And they calculated the electronic structure, the for-

*Project supported by the National Natural Science Foundation of China (Grant Nos 10744002 and 10774017).
†Corresponding author. E-mail: jun_chen@iapcm.ac.cn

mation energy of GB and the segregation energy of dopant. Recently, we also carried out a theoretical tensile experiment on Σ3 GB in alumina.[21] Our calculations showed that the Y–O bonding had a significant effect on the creep property of α-Al_2O_3.

The above experimental and computational results offer much insight into these points. However, it is not enough to perform the basic structure analysis of GB in alumina with dopant Y. As a result, the effects of dopant Y are not clearly understood. So, it is highly desirable to investigate these effects by using the general GB models that occur more frequently and are sensitive to the segregation of Y in real samples. One of general GBs, which have been experimentally studied, is the Σ37 GB in α-Al_2O_3. The experimentally observed dopant concentration of Y in the Σ37 GB attains to 4Y atoms/nm^2.[11] In the present paper, we give the results on the electronic structure of the Σ37 GB in α-Al_2O_3. The potential distribution, the effective charge and the bond order of ions are analysed in detail. Our purpose is to understand the 'Y-effect' in ceramic alumina. In the present paper, we employ the Vienna *ab initio* simulation package (VASP)[25] to study the GB structure. The remainder of the present paper is organized as follows. In Section 2, the methods and models are described. In Section 3, the calculated results are discussed in detail, and in Section 4 conclusions drawn from the present study are presented.

2. Computational approach and grain boundary model

The atomic structures of Σ37 GB with and without dopant Y are relaxed by using the VASP in the generalized gradient approximation (GGA-91) for the exchange potential.[25] We use both a plane wave basis set corresponding to an energy cutoff of 400eV and eight k points in the irreducible portion of the Brillouin Zone of the supercell. The total energy of system and the residual force on each atom converge to less than 0.001 eV and 0.1 eV/nm, respectively.

The relaxed $(01\bar{1}8)/[04\bar{4}1]/180°$ (Σ37) GB model is shown in Fig.1. This model has a total of 280 atoms (112 Al and 168 O ions) and two oppositely oriented GBs. The x-axis of this supercell is along the surface $(01\bar{1}8)$ direction of α-Al_2O_3. We then divide the model into four regions: two bulk regions and two GB regions as shown in Fig.1(a). The relaxed supercell parameters are a= 4.165 nm, b=0.471 nm, and c=1.173 nm. The GB has a cross-sectional area of 0.55283 nm^2. Each GB region contains 18 O and 12 Al ions. The statistical bond lengths and the neighbouring atom numbers are listed in Table 1. The coordination analysis shows that in the GB region, 12 Al ions are classified into four fivefold and eight sixfold Al ions, and 18 O ions can be identified as twelve fourfold and six threefold O ions. The longest and the shortest Al–O bonds in the GB region are 0.1992 nm

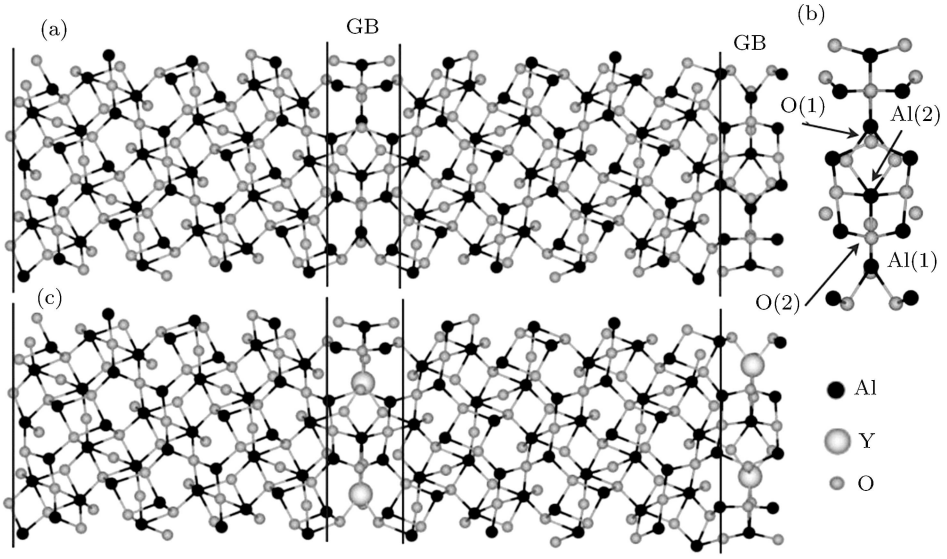


Fig.1. Relaxed models of clean and Y-doped Σ37 GBs in α-Al_2O_3, where panel (a) is for clean Σ37 GB; panel (b) for one of the GBs in panel (a), O(1) is 3-fold O, O(2) is 4-fold O, Al(1) is 5-fold Al and Al(2) is 6-fold Al; panel (c) for Y-doped Σ37 GB.

Table 1. Structure and bond analyses of clean and Y-doped Σ37 GBs, the averaged bond length (BL) and the nearest-neighbouring coordination of atom in GB region.

	lattice constant/nm			averaged BL/nm (bond order)		nearest-neighbour coordination			
	a	*b*	*c*	Al–O	Y–O	6-fold	5-fold	4-fold	3-fold
clean Σ37	4.165	0.471	1.173	0.1887(0.0162)		8Al	4Al	12O	6O
Y-doped Σ37	4.178	0.472	1.175	0.1867(0.0164)	0.1912(0.0162)	8Al	2Al, 2Y	12O	6O

and 0.1786 nm, respectively. The calculated GB formation energy is 0.79 J/m^2. For Y doping, two Y ions substitute two fivefold Al atoms in each GB region (seeing Fig.1(c)). It means that there are 4Y atoms, in total, doped in our studied model. The dopant concentration is consistent with the experimentally observed concentration of 4Y atoms/nm^2.[7] With Y-doped, the lattice constants have slightly changed just as shown in Table 1. The biggest Y–O bond is 0.2120 nm, and the smallest one is 0.1783 nm. The segregation energy $E_{\rm seg}$ of Y ion can be calculated by using the following formula:

$$E_{\rm seg} = (E_{\rm GB+Y} - E_{\rm GB}) - (E_{\rm bulk+Y} - E_{\rm bulk}), \quad (1)$$

where $E_{\rm GB+Y}$ and $E_{\rm GB}$ are the total energies of GB model with and without dopant Y, respectively, and $E_{\rm bulk+Y}$ and $E_{\rm bulk}$ are the energies of crystal model of alumina with and without dopant Y, respectively. The calculated segregation energy of Y ion in Σ37 GB in alumina is 2.37 eV/per atom.

In our calculation, the effective charge Q^*_α on each atom and the bond order $\rho_{\alpha,\beta}$ between each pair of atoms (α, β) are obtained from a separate minimal basis calculation based on Mulliken analysis by using the *ab initio* eigenvector coefficients $C^n_{i\alpha}$ and the overlapping integrals $S_{i\alpha,j\beta}$, where n is the band index

$$Q^*_\alpha = \sum_i \sum_{n,occ} \sum_{j,\beta} C^{*n}_{i\alpha} C^n_{j\beta} S_{i\alpha,j\beta}, \quad (2)$$

$$\rho_{\alpha\beta} = \sum_{n,\rm occ} \sum_{i,j} C^{*n}_{i\alpha} C^n_{j,\beta} S_{i\alpha,j\beta}. \quad (3)$$

3. Results and discussion

3.1. Electronic structure and environment of dopant

First, we calculate the electron density of states (DOS) of crystalline alumina. Here we do not plot the DOS of crystal alumina. The main characters of crystalline alumina are similar to those described in Ref.[26] and can be simplified as follows: the lower O(2s) states are located around –19 to –16 eV, and the O(2p) states constitute the upper valence band (VB) ranging from about –7 to 0 eV. Beyond Fermi level $E_{\rm g}$, the levels of Al(3s, 3p) constitute the conduction band (CB), and at the bottom of the CB, Al(3s) has the largest component. Our calculated band gap $E_{\rm g}$ is 6.2 eV, which is lower than the experimental value of 8.10 eV.[18] Such a discrepancy is expected when the DFT method is used.

Then, the model of Σ37 GB in alumina is studied. The total density of states (TDOS) and partial density of states (PDOS) of the Σ 37 GB model are shown in Fig.2. Just as defined in Fig.1(b), O(1) and

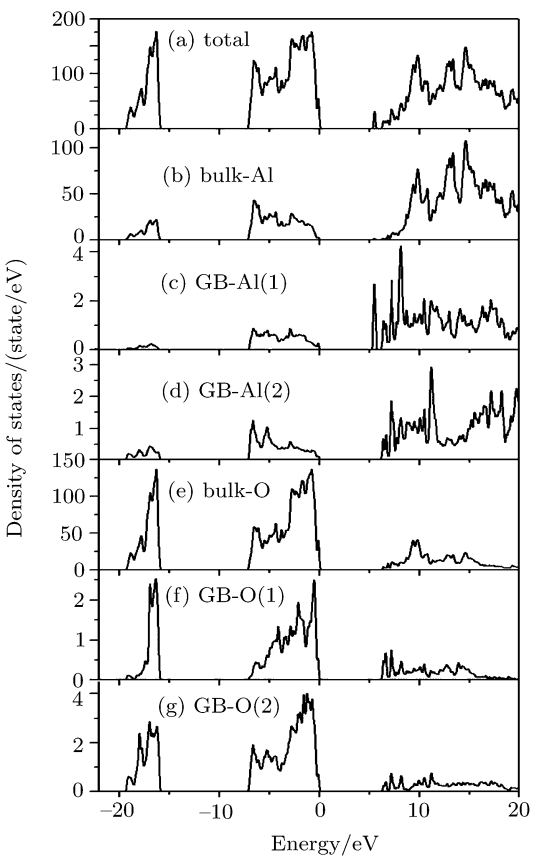


Fig.2. Calculated densities of states (DOSs) of clean Σ37 GB region, where panel (a) is for the total DOS of Σ37 GB region; panel (b) for the partial DOS of bulk Al atom; panel (c) for the partial DOS of 5-fold Al in GB region; panel (d) for the partial DOS of 6-fold Al in GB region; panel (e) for the partial DOS of bulk O atom; panel (f) for the partial DOS of 3-fold O in GB region; panel (g) for the partial DOS of 4-fold O in GB region.

O(2) mean the threefold O and the fourfold O, Al(1) and the Al(2) mean the fivefold Al and sixfold Al in the GB region, respectively. Compared with the band gap of 6.2 eV of the crystalline alumina, the band gap of the Σ37 GB is reduced to 5.2 eV. The PDOSs of O and Al at different sites are also shown in Figs.2(b)-to-2(f). It is clearly shown that the threefold O and the fourfold O in the GB region have different patterns. For the threefold O, DOS has three peaks in the first VB. But, the fourfold O has a state nearly similar to the state that bulk O has. And Al(1) and Al(2) also have different states in the conduction band. Now, the edge of CB is composed of the fivefold Al(1) states, and it is at lower energy level than the edge of CB composed of bulk Al states. This is the reason why the Σ 37 GB model has a reduced band gap compared with that in crystalline alumina.

After Y-doped in GB, the Y ion induces new energy levels near the bottom of CB and in the second VB. The TDOS and the PDOS of relatively atoms are plotted in Fig.3. Now, the Y(4d) state constitutes the edge of CB and results in a smaller band gap 4.5eV of Σ37 GB with dopant Y. Comparing the PDOS of Y ion with the TDOS (see Figs.(3a) and (3d)), we can find that the peaks of Y(4p) and Y(3d) both are located about at E=–20 eV, and there is a strong overlapping and hybridization between state of Y(4p) or Y(3d) and that of O(2s). The bonding of Y–O stronger than that of Al–O as analysed later can be caused by this hybridization. Moreover, Y-doping leads to the changes of PDOS of the threefold O(1) and the fourfold O(2) as compared with clean GB just as shown in Figs.3(f) and 3(g). The O(1) and O(2) both show a wider second VB after Y-doping.

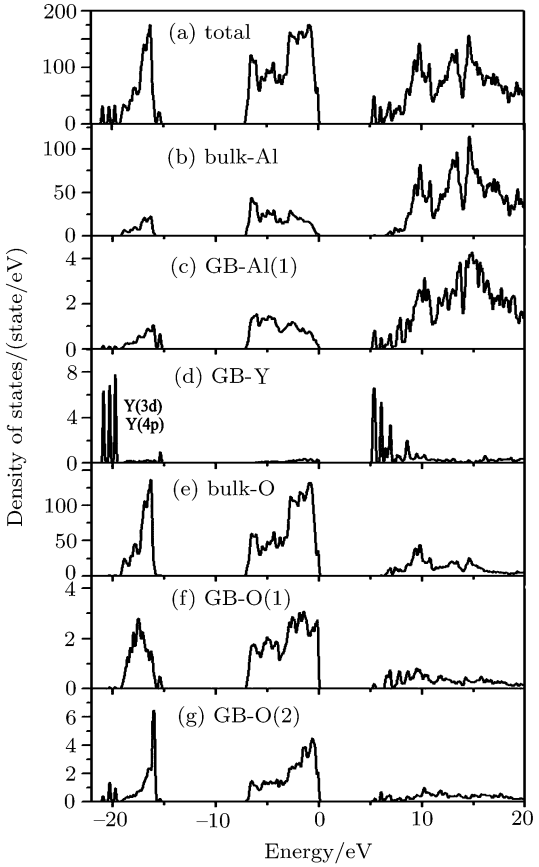


Fig.3. Calculated densities of states(DOSs) of Y-doped Σ37 GB region, where panel (a) is for the total DOS of Y-doped Σ37 GB region; panel (b) for the partial DOS of bulk Al atom; panel (c) for the partial DOS of 6-fold Al in GB region; panel (d) for the partial DOS of 5-fold Y in GB region; panel (e) for the partial DOS of bulk O atom; panel (f) for the partial DOS of 3-fold O in GB region; panel (g) for the partial DOS of 4-fold O in GB region.

Figure 4 shows the VASP calculated electrostatic potential $V(\boldsymbol{r})$, which is acquired through the numerical solution of the Poisson equation on a fine grid of 360×84×108. It can be seen in Fig.4(a) that in the bulk region of the clean Σ37 GB model, the potential varies from –1.5 eV to 1.0 eV, but in the GB region, the potential varies from –3.9 to 2.0 eV. If we calculate the average potentials of different regions, we can find that there is a potential difference of about 0.1 eV between the GB region and the bulk region. This potential difference will induce an uneven charge distribution in the GB region (see Fig.4(a)). The lowest potential is in the central part of GB region. And near the interface between the bulk region and the GB region, there is the biggest potential distribution. After Y doping (see Fig.4(b)), the potential in the central part of GB region increases and the difference in potential between the GB region and the bulk region attains up to 0.6 eV. The larger difference in potential indicates that Y-doping results in an accumulation of more charges in the GB region. We also see that the potential distributions of two GB regions are not identical. This is may be due to the fact that our grain boundary model has a slightly difference between before and after relaxation.

The electrostatic potential distribution in the GB region has some relevance to the space charge model (SCM) in ceramic insulators, which was proposed long ago.[27] The SCM is the central theme for explaining many transport behaviours such as solute segregation in ceramics that contains microstructures, defects and impurities.[28,29] Strictly speaking, the SCM is an empirical theory based on a formal charge description of the ionic species and defect formation energies derived

from indirect experimental measurements.[30] In the GB or other defective structure, oppositely charged ions are unbalanced. The accumulation of like sign charges must be balanced by space charges of the opposite sign. Our results about potential reveal that the Y dopant will affect the space charge distribution in the GB. After Y-doping, more charges will accumulate on the interface of GB, and so the transport property of ceramics will be affected.

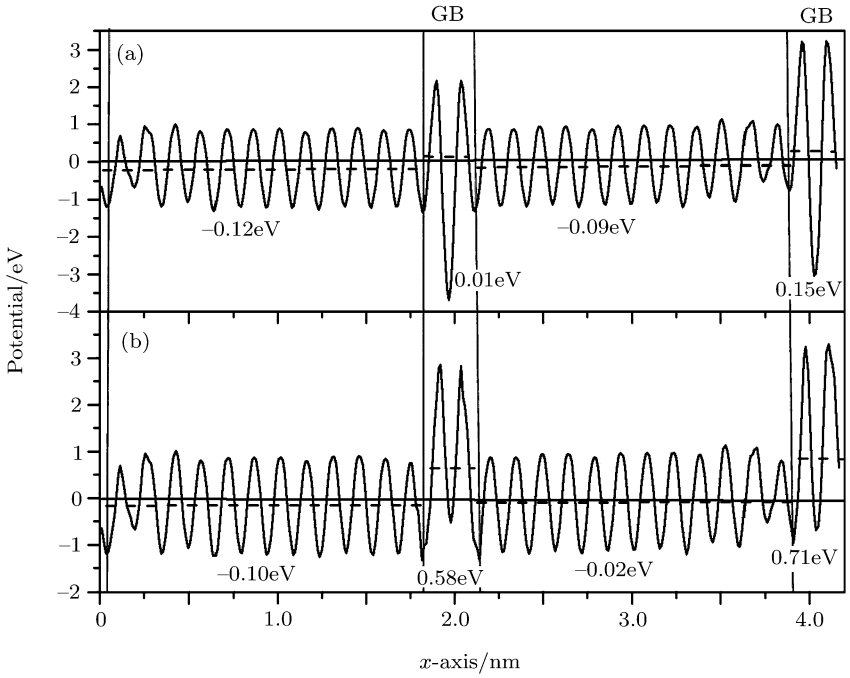


Fig.4. Calculated electrostatic potentials along the x-direction in (a) clean Σ37 GB region and (b) Y-doped Σ37 GB region separately.

3.2. Bond order and effective charge of GB

Figure 5 shows the averaged bond order of each atom in the Σ37 GB model with and without Y-doping. The bond order of each atom is the average of all bonds where the atom bonds to its neighbouring atoms. For the clean GB model (see Fig.5(a)), we find that Al and O ions in the bulk region have almost identical values of bond order. But, in the GB region, the bond order of Al (O) ion varies from 0.158 (0.163) to 0.202 (0.201). In the GB region, threefold O has the smallest bond order, 0.163, among all O ions, and the fivefold Al has the smallest bond order, 0.158, among all Al ions. Near the GB interface, the Al atom displays a bigger bond order than in the bulk region. After Y doping just as shown in Fig.5(b), the Y substitutes the fivefold Al, which has the smallest bond order among Al ions in the GB region. Comparing the bond order of 4 Y–O bonds and the replaced 4 Al–O bonds, the Y–O bond order has an averaged value of 0.163, and the replaced Al–O bond order is 0.160. This indicates that Y–O bond has a higher strength than the replaced Al–O bond. As analysed in the PDOS above, the stronger Y–O bond is due to the hybridization of Y(4p, 3d) with O(2s) orbital. Moreover, the Al ion in the centre of GB region displays weaker bond order than near the interface. This is due to the fact that the 5-fold Al ions are located mainly in the central part of GB region. As pointed in Ref.[21], the fracture of material is determined by the weakest bond. So, we can reasonably predicate that the bond distortion starts from a weaker fivefold Al–O bond in a central part of Σ37 GB region. Yet, after Y-doping, the stronger Y–O bond will reinforce the GB.

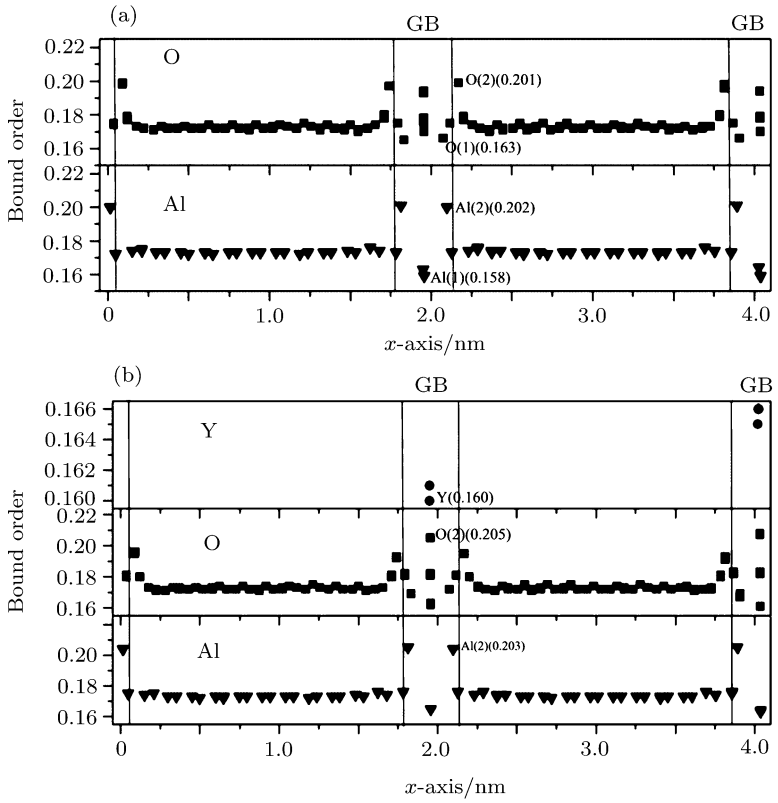


Fig.5. Calculated bond orders of atom in (a) clean Σ37 GB region and (b) Y-doped Σ37 GB region separately.

Figure 6 shows the calculated values of Mulliken effective charge Q^* for all the atoms in the Σ37 GB model with and without dopant Y. For the clean GB model (see Fig.6(a)), effective charges vary from $6.83e$ to $7.04e$ ($1e = 1.6 \times 10^{-19}$C) for the O ions and from $7.49e$ to $7.77e$ for the Al ions. In the bulk region, there is a small range of distributions for either cations or anions. In the GB region, the threefold O(1) ions have, as expected, a slightly smaller value of Q^*. This slight change in Q^* could also be due to the changes in the Al–O bond-length and the coordination number of threefold O in the GB region as listed in Table 1. After Y doping (see Fig.6(b)), the averaged effective charge of 4 Y atoms is $7.898e$ bigger than that of replaced 4 fivefold Al(1) ions. This is consistent with the fact that the Y–O bond is stronger than replaced Al–O bond.

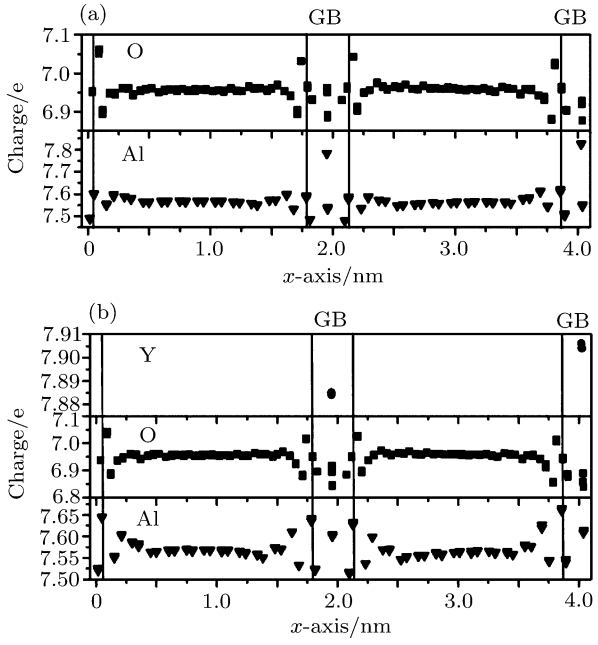


Fig.6. Calculated effective charges of atom in (a) clean Σ37 GB region and (b) Y-doped Σ37 GB region separately.

4. Conclusions

In the present paper, the electronic structures of Σ37 GB with and without dopant Y are studied by using the VASP. The potential distribution, the bond order and the effective charge are calculated. Our results clearly demonstrate that the Y–O bond is stronger than the replaced Al–O bond. This may be due to the hybridization of Y(4p,3d) with the O(2s) orbital. Moreover, Y doping also affects the potential distribution in the GB region. The difference in potential between the GB region and the bulk region is larger after Y-doping than before. It implicitly interprets that Y-doping will affect the transport property of ceramic alumina.

Acknowledgment

The initial model of this work was finished during the corresponding author was working in the group of W Y Ching at the University of Missouri Kansas City (UMKC), USA. The resources of Shenteng-6800 used in this work were supported by the Supercomputing Centre of Chinese Academy of Sciences (SCCAS).

References

[1] Atsunaga K, Nishimura H, Muto H, Yamamoto T and Ikuhara Y 2003 *Appl. Phys. Lett.* **82** 1179
Nishimura H, Matsunaga K, Sato T, Yamamoto T and Ikuhara Y 2003 *J. Am. Ceram. Soc.* **86** 574
[2] Li Y, Wang C M, Chan H M, Rickman J M, Harmer M P, Chabala J M, Gavrilov K L and Levi Setti R 1999 *J. Am. Ceram. Soc.* **82** 1497
[3] Thompson A M, Soni K K, Chan H M and Harmer M P 1997 *J. Am. Ceram. Soc.* **80** 373
[4] Cook R F and Schrott A G 1988 *J. Am. Ceram. Soc.* **71** 50
[5] Taylor R I, Cood J P and Brook R J 1974 *J. Am. Ceram. Soc.* **57** 539
[6] Lartigue S, Priester L, Dupan F, Gruflel P and Carry C 1993 *Mater. Sci. Eng.* A **164** 211
[7] Le Gall M, Huntz A M, Lesage B, Monty C and Bernadini J 1995 *J. Mater. Sci.* **30** 201
[8] Bouchet D, Dupau F and Lartigue-Korinel S 1993 *Microsc Microanal Microstruct.* **4** 561
[9] Gülgün M A, Putlayev Valery and Rühle Manfred 1999 *J. Am. Ceram. Soc.* **82** 1849
[10] Wang C M, Cargill G S, Chan H M and Harmer M P 2000 *Acta Mater.* **48** 2579
[11] Gemming T, Nufer S, Kurtz W and Rühle M 2003 *J. Am. Ceram. Soc.* **86** 590
[12] Voytovych R, Maclaren I, Gulgun M A, Cannon R M and Ruhle M 2002 *Acta Mater.* **50** 2453
[13] Bruley J, Cho J, Chan H M, Harmer M P and Rickman J M 1999 *J. Am. Ceram. Soc.* **82** 2865
[14] Cho J, Chan H M, Harmer M P, Rickman J M and Thompson A M 1998 *J. Am. Ceram. Soc.* **81** 3001
[15] Cho J, Chan H M, Rickman J M and Harmer M P 2000 *J. Am. Ceram. Soc.* **83** 344
[16] Port D, Gall M Le, Lesage B, Huntz A M and Monty C 1996 *Philos. Mag.* A **73** 935
[17] Lu G H, Deng S H, Wang T M, Kohyama Masanori and Yamamoto Ryoichi 2004 *Phys. Rev.* B **69** 134106
[18] Ching W Y and Xu Y N 1999 *Phys. Rev.* B **59** 12815
[19] Elsasser C and Elsasser T 2005 *J. Am. Ceram. Soc.* **88** 1
[20] Elsasser C and Marinopoulos A G 2001 *Acta Mater.* **49** 2951
[21] Chen J, Xu Y N, Rulis Paul, Ouyang L and Ching W Y 2005 *Acta Mater.* **53** 403
[22] Zhang Y, Lu G H, Deng S H and Wang T M 2007 *Phys. Rev.* B **75** 174101
[23] Lu G H, Zhang Y, Deng S H, Wang T M, Kohyama M, Yamamoto R, Liu F, Horikawa K and Kanno M 2006 *Phys. Rev.* B **73** 224115
[24] Lu G H, Deng S H, Wang T M, Kohyama M and Yamamoto R 2004 *Phys. Rev.* B **69** 134106
[25] Kresse G and Furthmuller J 1996 *Phys. Rev.* B **54** 11169
[26] Matsunaga K, Tanaka T, Yamamoto T and Ikuhara Y 2003 *Phys. Rev.* B **68** 85110
[27] Kingery W D 1974 *J. Am. Ceram. Soc.* **57** 1
[28] Ikeda J A S and Chiang Y M 1993 *J. Am. Ceram. Soc.* **76** 2437
[29] Ikeda J A S, Chiang Y M, Garratt-Reed A J and Vander Sande J B 1993 *J. Am. Ceram. Soc.* **76** 2447
[30] Kliewer K L and Kohler J S 1965 *Phys. Rev.* **140** A1226